

Statistics of Fourier Modes of Velocity and Vorticity in Turbulent Flows: Intermittency and Long-Range Correlations

L. Chevillard, N. Mazellier, C. Poulain, Y. Gagne, and C. Baudet

Laboratoire des Ecoulements Géophysiques et Industriels, BP53, 38000 Grenoble, France

(Received 7 June 2005; published 11 November 2005)

We perform a statistical analysis of experimental fully developed turbulence longitudinal velocity data in the Fourier space. We address the controversial issue of statistical intermittency of spatial Fourier modes by acting on the finite spectral resolution. We derive a link between velocity structure functions and the flatness of Fourier modes thanks to cascade models. Similar statistical behaviors are recovered in the analysis of spatial Fourier modes of vorticity obtained in an acoustic scattering experiment. We conclude that vorticity is long-range correlated and found more intermittent than longitudinal velocity.

DOI: [10.1103/PhysRevLett.95.200203](https://doi.org/10.1103/PhysRevLett.95.200203)

PACS numbers: 47.27.Gs, 02.50.Fz, 43.58.+z

In fully developed turbulence, most of the experimental, numerical, and theoretical works [1] focus on the statistics of the longitudinal velocity increments $\delta_r u(x) = u(x+r) - u(x)$. It is now well established that structure functions $M_q(r) = \langle (\delta_r u)^q \rangle_x$, behave as power laws, i.e., $M_q(r) \sim r^{\zeta_q}$. The universal nonlinear evolution of ζ_q with respect to q is referred to the so-called intermittency phenomenon: the probability density function (PDF) of velocity u is close to Gaussian, while the PDF of longitudinal velocity gradients $\partial_x u$ exhibits extremely large tails. Another striking property of turbulence is the long-range correlation of dissipation events, i.e., $(\partial_x u)^2$, up to the velocity correlation length scale L . Many systems share the same types of behaviors, as financial volatility [2] and electrical transport in granular media [3]. A major issue in turbulence is to derive a possible link between long-range correlations and vorticity filaments [4]. In the Fourier space, which is an alternative way to study turbulence statistics [5], one could expect that the Fourier modes of velocity $\tilde{u}(k, t)$ should analogously follow the same types of behaviors, i.e., $\langle |\tilde{u}(k, t)|^q \rangle_t \sim k^{-\zeta_q}$, since k can be interpreted as the inverse of a scale, as prescribed in shell models [6]. Furthermore, a statistical model based on the rapid distortions of the small scales predicts strong intermittency in the k space [7]. Surprisingly, it is not the case on experimental and numerical velocity profiles, as pointed out by the seminal paper of Brun and Pumir [8], since the PDFs of Fourier modes are found to be undistinguishable from Gaussians, whatever the value of k .

However, one of the crucial parameters of the Fourier transform is the finite spectral resolution associated with the finite length of velocity profiles hereafter noted ℓ . The goal of this Letter is to show that, whereas statistics of Fourier modes do not depend on k , they depend significantly on the ratio ℓ/L . First, we present such a “short-time” Fourier analysis of experimental longitudinal velocity data. Second, the statistical dependence on ℓ/L is clarified in the context of various turbulent cascade models. Finally, we perform a similar analysis on experimental

data, obtained in an acoustic scattering experiment, allowing the direct probing in time of spatial Fourier modes of vorticity in a turbulent air jet. By comparison with the longitudinal velocity data analysis, we conclude that vorticity is also long-range correlated but more intermittent.

Let us introduce the short-time Fourier analysis $\tilde{u}_\ell(k, x)$, which depends on the space variable x and the wave vector k and corresponds to the computation of the Fourier transform of the longitudinal velocity $u(x)$ in a window h_ℓ of size ℓ , i.e., $\tilde{u}_\ell(k, x) = u(x) \otimes [e^{-ikx} h_\ell(x)]$, where \otimes stands for the convolution product. We represent in Fig. 1(a) the flatness of $|\tilde{u}_\ell(k, x)|$, i.e., $\mathcal{F}_\ell(k) = \langle |\tilde{u}_\ell(k, x)|^4 \rangle / \langle |\tilde{u}_\ell(k, x)|^2 \rangle^2$, as a function of $\ln(k/k_\eta)$, where $k_\eta = (\eta_K)^{-1}$ (η_K is the dissipative Kolmogorov length scale), for several windowing length ℓ (see the caption), and for $k \geq 2\pi/\ell$. The experimental longitudinal velocity signal used in this study has been recorded in the Modane’s wind tunnel facility [9] at a Taylor microscale Reynolds number $\mathcal{R}_\lambda \approx 2500$ and thus exhibits a large inertial range. Here, the spectral window is the Hanning function: $h_\ell(x) = \cos^2(\pi x/\ell)$ for $x \in [-\ell/2, \ell/2]$, $h_\ell(x) = 0$ instead. For inertial wave vectors ($k < k_\eta$), $\mathcal{F}_\ell(k)$ slightly depends on k but drastically on ℓ : when ℓ is of the order of several correlation lengths ($\ell \gg L$), $\mathcal{F}_\ell(k)$ is close to the Gaussian value 2 [as found in [8]] and when $\ell/L \rightarrow 0$, we note a rapid increase of the value of this inertial “plateau.” The evolution of $\mathcal{F}_\ell(k)$ with respect to ℓ/L is displayed on Fig. 1(c). The error bars have been obtained by a least-square fit of the plateaus of the flatness over wave vectors in the inertial range. We thus observe that the flatness of the Fourier modes behaves as a power law of the scale ℓ , i.e., $\mathcal{F}_\ell(k) \sim \ell^\alpha$ with $\alpha = -0.1 \pm 0.02$. Here, the error bar 0.02 is large because of the lack of statistics and the fact that longitudinal velocity profiles, obtained under the Taylor hypothesis [1], are sensitive to the temporal decorrelation [10]. We have also displayed in Fig. 1(c) the evolution of the flatness for another longitudinal velocity profile ($\mathcal{R}_\lambda \approx 300$) obtained in the air jet we will present at the end of this Letter. Hence, α remains

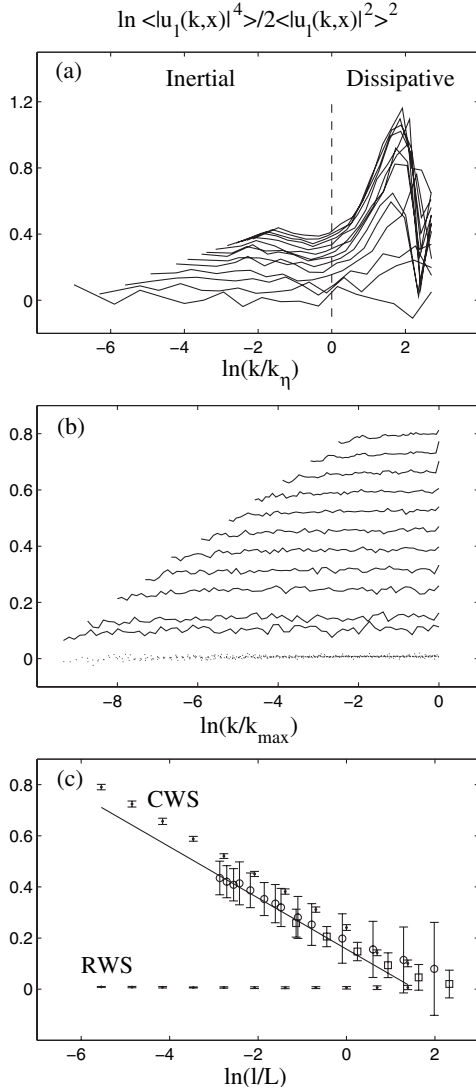


FIG. 1. (a) Flatness of $|\tilde{u}_\ell(k, x)|$ as a function of $\ln(k/k_\eta)$ [$k_\eta = (\eta_R)^{-1}$], for different window lengths ℓ (from top to bottom, $\ell/L = 0.057; 0.067; 0.078; 0.089; 0.114; 0.156; 0.200; 0.228; 0.334; 0.456; 0.91; 1.82; 3.64; 7.28$) for the Modane velocity signal ($\mathcal{R}_\lambda \approx 2500$). (b) Flatness of synthetic velocity profiles $|\tilde{u}_\ell^{\text{RWS}}(k, x)|$ (dotted line) and $|\tilde{u}_\ell^{\text{CWS}}(k, x)|$ (solid line) vs $\ln(k/k_{\text{max}})$, where k_{max} is the Nyquist wave vector and for several scales [from top to bottom $\log_2(\ell_p/L) = -8, -7, -6, -5, -4, -3, -2, -1, 0, 1$ and 2]. (c) Values of the plateaus of parts (a) and (b) vs $\ln(\ell/L)$: (○) modane velocity data, (□) air-jet velocity data ($\ell/L = 0.32; 0.64; 1.28; 2.56; 5.12; 10.24$), (●) synthetic velocities, (solid line) our theoretical prediction [Eq. (3)].

unchanged and can be considered as universal. Let us mention that the second moment of $|\tilde{u}_\ell(k, x)|$ is obviously proportional to $k^{-5/3}$ and $\langle |\tilde{u}_\ell(k, x)|^2 \rangle = (\ell/L) \langle |\tilde{u}_L(k, x)|^2 \rangle$ for $k \geq 2\pi/\ell$. In the dissipative range (i.e., $k > k_\eta$), the flatness appears to rapidly increase without any saturation [11]. This is one of the first experimental verifications of a Kraichnan's conjecture [12,13] which is linked to the log-

infinitely distribution breaking of velocity [14] and is currently under investigation. In the following, we will theoretically establish a link between the inertial exponent α and the structure function exponent ζ_q : $\alpha = \zeta_4 - 2\zeta_2$.

Let us now begin with defining an intermittent (zero mean) velocity profile. This is usually done with the help of wavelet series [15], early introduced in the context of turbulence [16,17],

$$u(x) = \sum_{j=0}^{+\infty} \sum_{k=0}^{2^j-1} c_{j,k} \psi_{j,k}(x), \quad (1)$$

where the set $\{\psi_{j,k}(x) = 2^{j/2} \psi(2^j x - k)\}$ is an orthonormal basis of the space of finite energy functions $L^2([0, L])$ [see [18]] and ψ an admissible “mother” wavelet. The wavelet coefficients $c_{j,k}$ govern the statistics across scales. Generally, the coefficients $c_{j,k} = 2^{-j/2} \epsilon_{j,k} \beta_{j,k}$ are chosen as a product of a sign ($\epsilon_{j,k} = \pm 1$ with equal probability) and positive random variables $\beta_{j,k}$ that are chosen so as to be compatible with turbulence longitudinal velocity statistics, i.e., $\mathbb{E}(\beta_{j,k}^q) = 2^{-j\zeta_q}$ [$\mathbb{E}(\cdot)$ meaning here mathematical expectation]. Moreover, as already predicted by the unifying point of view of Cates and Deutsch [19], statistics of velocity fluctuations are correlated in space and scale that can be formalized through space-scale correlations of dyadic wavelet coefficients as $\mathbb{E}(\beta_{j,k}^{q_1} \beta_{l,m}^{q_2}) = \mathbb{E}(\beta_{j,k}^{q_1}) \mathbb{E}(\beta_{l,m}^{q_2}) C_{j,k,l,m}^{q_1,q_2}$, where the functions $C_{j,k,l,m}^{q_1,q_2}$ render additional correlations

$$C_{j,k,l,m}^{q_1,q_2} = [|k2^{-j} - m2^{-l}| + \max(2^{-j}, 2^{-l})]^{\zeta_{q_1+q_2} - \zeta_{q_1} - \zeta_{q_2}} \quad (2)$$

stating that wavelet coefficients are typically correlated, in amplitude, up to the correlation length L . The generated velocity profile $u^{\text{CWS}}(x)$ using Eq. (1), where $\beta_{j,k}$ are correlated according to Eq. (2), will be called a *cascade wavelet series* (CWS) [8,17,18]. Using the simplest admissible Haar wavelet [i.e., $\psi(x) = 1$ for $x \in [0; L/2]$, $\psi(x) = -1$ for $x \in [L/2; L]$, $\psi(x) = 0$ instead] and the box for the short-time Fourier transform [i.e., $h_\ell(x) = 1$ for $x \in [0; \ell]$, and $h_\ell(x) = 0$ instead], it can be shown analytically that $\mathbb{E}[|\tilde{u}_{\ell_p}^{\text{CWS}}(k_n, 0)|^2] \propto (\ell_p/L) k_n^{-1-\zeta_2}$, for $k_n = \pi 2^n / L > \pi/\ell_p$ and $\ell_p = L 2^{-p}$ [$(n, p) \in \mathbb{N}^2$]. Moreover, the flatness $\mathcal{F}_{\ell_p}(k_n) = \mathbb{E}[|\tilde{u}_{\ell_p}^{\text{CWS}}(k_n, 0)|^4] / (\mathbb{E}[|\tilde{u}_{\ell_p}^{\text{CWS}}(k_n, 0)|^2])^2$ behaves as

$$\mathcal{F}_{\ell_p}(k_n) = 2 \frac{2}{(1 + \zeta_4 - 2\zeta_2)(2 + \zeta_4 - 2\zeta_2)} \left(\frac{\ell_p}{L}\right)^{\zeta_4 - 2\zeta_2} \quad (3)$$

when $\ell_p \rightarrow 0$ independently of k_n . We thus have demonstrated that $\alpha = \zeta_4 - 2\zeta_2$. Note that the flatness is not exactly equal to 2 at the correlation length ($\ell_p = L$).

In order to check our analytical predictions, in particular, to verify whether our computations depend on the box h_ℓ

and the synthesis wavelet ψ , we perform a statistical study of the process $u^{\text{CWS}}(x)$, using a more regular Daubechies-6 wavelet for the synthesis wavelet ψ and a Hanning window for h_ℓ . The method used to build the positive random variables $\beta_{j,k}$ is the classical multiplicative cascade model [8,17–21]: recursively, $\beta_{0,0} = 1$, $\beta_{j,2k} = W_{j-1,k}^{(l)} \beta_{j-1,k}$, and $\beta_{j,2k+1} = W_{j-1,k}^{(r)} \beta_{j-1,k}$, where the $W_{j-1,k}^{(\kappa)}$ ($\kappa = l$ for left or r for right) are independent identically distributed (IID) positive random variables [see [17,18]]. As an example, we will study the log-normal case where each $\ln W_{j-1,k}^{(\kappa)}$ is a Gaussian random variable of mean $\mu \ln 2$ and variance $\sigma^2 \ln 2$ (leading to the quadratic spectrum $\zeta_q = \mu q - \sigma^2 q^2/2$). We have used the set of parameters $\sigma^2 = 0.025$ and $\mu = 1/3 + 3\sigma^2/2$, consistent with experimental findings [22], so that $\zeta_2 \approx 2/3$, $\zeta_3 = 1$, and $2\zeta_2 - \zeta_4 = 0.1$. Numerically, the infinite sum in Eq. (1) is truncated at $j = N = 2^{18}$ and is generated over 2^5 integral scales. It can be shown that such a stochastic process is not stationary [23] but at first order, its correlation function is consistent with Eq. (2). We show in Fig. 1(b) (solid line) the estimation of the flatness of $\tilde{u}_{\ell_p}^{\text{CWS}}(k, x)$ as a function of $\ln(k/k_{\text{max}})$. After a k -dependent crossover (data not shown) linked, among other reasons, to the effect of discreteness in the cascade [21], the flatness does not depend on the wave vector k but significantly depends on ℓ_p . In Fig. 1(c), we have gathered all the values of the inertial plateaus using a least-square fit providing an error bar estimation. The plateau behaves as a power law of the scale ℓ_p in accordance with Eq. (3): $\zeta_4 - 2\zeta_2 = -0.1 \pm 0.001$. The discrepancies between the prefactors are mainly linked to the nonstationary character of this generated synthetic velocity profile.

We would like to mention that if wavelet coefficients are no longer long-range correlated (take $C_{j,k,l,m}^{q_1,q_2} = 1$) and if $\ln \beta_{j,k}$ are chosen to be independent Gaussian random variables with mean $\mu \ln 2^j$ and variance $\sigma^2 \ln 2^j$, the corresponding synthetic velocity generated will be called a *random wavelet series* (RWS) $u^{\text{RWS}}(x)$ which is intermittent in a mathematical sense [24]. By construction, $\mathbb{E}[|\tilde{u}_{\ell_p}^{\text{CWS}}(k_n, 0)|^2] = \mathbb{E}[|\tilde{u}_{\ell_p}^{\text{RWS}}(k_n, 0)|^2]$, and analytical calculations performed in the same framework defined in the context of CWS (i.e., using a Haar wavelet for ψ and a box for h_ℓ) show that the flatness $\mathcal{F}_p(k_n)$ is equal to 2 for both wave vectors k_n and window lengths ℓ_p . This property has been checked numerically (with the same parameters μ and σ , and the same synthesis wavelet ψ and analysis window h_ℓ as in the CWS case). The results are presented in Figs. 1(b) and 1(c). This heuristic synthetic process shows that experimental longitudinal velocity data are not only intermittent, but also long-range correlated.

We will turn now to acoustic scattering measurements allowing the direct access to a spectral characterization of

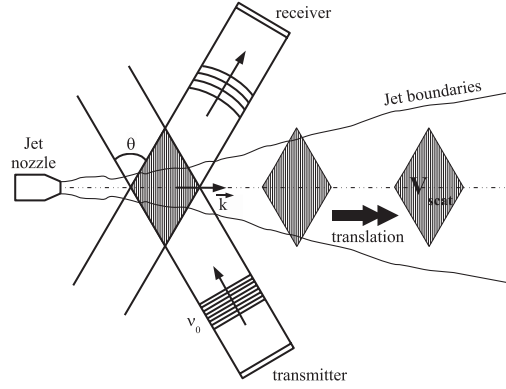


FIG. 2. Acoustic scattering experiment in a turbulent jet flow.

the vorticity distribution. The nonlinear interaction of an acoustic wave with a turbulent flow gives rise to a scattering process of the incident sound wave by the turbulent vorticity distribution. As in any scattering experiment (like, e.g., light or neutron scattering), the complex amplitude of the scattered acoustic pressure field is directly related to the incident acoustic amplitude and to the spatial Fourier transform of the vorticity distribution [25]. We have performed such a spectral investigation on a turbulent axisymmetric jet in air, at a Taylor-based Reynolds number $R_\lambda \approx 300$. We use a bistatic configuration (Fig. 2) wherein a plane monochromatic acoustic wave with frequency ν_0 and complex amplitude $p_{\text{inc}}(t)$ is directed on the turbulent flow. The complex amplitude $p_{\text{scatt}}(t)$ of the sound wave scattered at angle θ is then recorded along time by a separate acoustic receiver. Further details of the experimental apparatus can be found elsewhere [26]. The scattering process results in phase and amplitude modulations of the scattered acoustic pressure with respect to the incident one: $p_{\text{scatt}}(t) = \tilde{\Omega}_\perp(\vec{k}, t) p_{\text{inc}}(t)$, where

$$\tilde{\Omega}_\perp(\vec{k}, t) = \iiint_{V_{\text{scatt}}} \Omega_\perp(\vec{x}, t) e^{-i\vec{k}\cdot\vec{x}} d^3x \quad (4)$$

is the spatial Fourier transform of the vorticity component normal to the scattering plane at wave vector \vec{k} such that $|\vec{k}| = 4\pi\nu_0/c \times \sin(\theta/2)$, with c the sound speed. By fixing both ν_0 and θ , the scattering experiment allows the direct probing, in time, of a well-defined spatial Fourier mode of the turbulent vorticity distribution characterized by a unique spatial wave vector \vec{k} (spectral resolution). The price to pay for such a spectral resolution lies in some spatial delocalization in the physical space manifesting itself as a windowed spatial Fourier transform over a finite volume V_{scatt} according to Eq. (4). The measurement volume is defined by the intersection of the incident and detected acoustic beams and mainly depends on θ and on the size of both acoustic transducers. In the present experiment, $\theta = 60^\circ$ and the diameter of the circular transducers is 14 cm, leading to spatial resolutions of order the integral length scale of the jet flow L . By varying

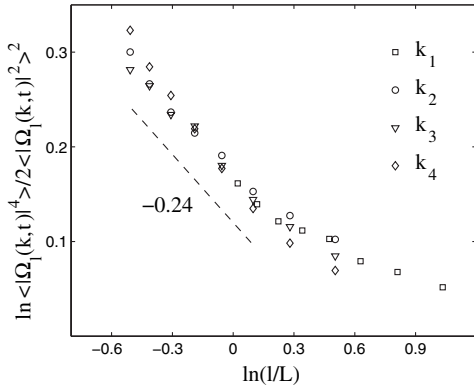


FIG. 3. Flatness of experimental Fourier modes of vorticity vs $\ln(\ell/L)$, for four inertial wave vectors k_i . Dotted line slope is equal to -0.24 .

ν_0 , at a fixed θ , four different wave vectors k_i , $i = 1, 2, 3, 4$ (in growing order) have been analyzed, corresponding to various length scales spanning the whole inertial range of the turbulent flow. In the spirit of the first part of this Letter, we are interested in the influence of the parameter ℓ/L where $\ell \sim (V_{\text{scat}})^{1/3}$ is a typical size of the measurement volume and L is the integral scale of the flow over the flatness $\mathcal{F}_\ell(k_i) = \langle |\Omega_\ell(\vec{k}, t)|^4 \rangle_t / \langle |\Omega_\ell(\vec{k}, t)|^2 \rangle_t^2$. To this end, we rely on the classical self-similarity property of the axisymmetric turbulent jet [27] according to which the integral scale L (and all other pertinent scales) increases linearly with respect to the distance downstream from the jet nozzle. A well-known consequence of this statistical self-similarity is the invariability of the Reynolds number for large enough distances from the jet nozzle. Several scattering experiments have been performed at different distances from the jet nozzle, corresponding to different integral length scales L . On Fig. 3 is plotted the flatness of the modal amplitude $\mathcal{F}_\ell(k_i)$ as a function of $\ln(\ell/L)$. First, $\mathcal{F}_\ell(k_i)$ does not depend on the wave vector k_i at a first order for $\ell < L$, in accordance with Fig. 1(c). Second, we see that the flatness behaves as a power law with scale ℓ , i.e., $\mathcal{F}_\ell(k_i) \sim \ell^\gamma$ with $\gamma = -0.24 \pm 0.02$ when $\ell/L \rightarrow 0$. Analogously with longitudinal velocity, the exponent γ is directly related to the classical ζ_q^Ω exponent of structure functions of vorticity considered as a vector field, namely $\gamma = \zeta_4^\Omega - 2\zeta_2^\Omega$. It is noticeable that our experimental finding is in excellent agreement with a tensorial wavelet analysis of Kestener and Arneodo [28] that has been applied to a 3D-vorticity field obtained from a direct numerical simulation (DNS) of Navier-Stokes equations at a smaller Reynolds number $\mathcal{R}_\lambda = 140$ for which they obtained $\zeta_4^\Omega - 2\zeta_2^\Omega = -0.22 \pm 0.016$. In the same spirit, it has been measured that transverse velocity profiles are more intermittent than longitudinal ones [29].

To sum up, we have shown that longitudinal velocity and vorticity are intermittent and long-range correlated in the physical space thanks to the study of the flatness of experi-

mental velocity data and acoustical measurements of vorticity Fourier modes. We have seen that vorticity is much more intermittent than longitudinal velocity. Our theoretical study on wavelet series shows that the intermittency is intrinsically related to long-range correlations. We mention the necessity to generalize this approach to dissipative length scales and wave vectors for which log-infinitely divisible principles are violated.

This work is supported by the French Research Ministry, Joseph Fourier University (PPF plateforme expérimentale de spectroscopie acoustique multi-échelles), and the CNRS. We wish to acknowledge B. Lashermes and P. Borgnat for useful comments.

- [1] U. Frisch, *Turbulence* (Cambridge University Press, Cambridge, England, 1995).
- [2] I. Giardina *et al.*, *Physica* (Amsterdam) **299A**, 28 (2001).
- [3] E. Falcon *et al.*, *Europhys. Lett.* **65**, 186 (2004).
- [4] F. Moisy and J. Jiménez, *J. Fluid Mech.* **513**, 111 (2004).
- [5] S. K. Dhar *et al.*, *Phys. Rev. Lett.* **78**, 2964 (1997).
- [6] L. Biferale, *Annu. Rev. Fluid Mech.* **35**, 441 (2003).
- [7] B. Dubrulle *et al.*, *J. Fluid Mech.* **520**, 1 (2004).
- [8] C. Brun and A. Pumir, *Phys. Rev. E* **63**, 056313 (2001).
- [9] H. Kahalerras *et al.*, *Phys. Fluids* **10**, 910 (1998).
- [10] B. Castaing, *Eur. Phys. J. B* **29**, 357 (2002).
- [11] L. Chevillard *et al.*, *Eur. Phys. J. B* **45**, 561 (2005).
- [12] R. H. Kraichnan, *Phys. Fluids* **10**, 2080 (1967).
- [13] U. Frisch and R. Morf, *Phys. Rev. A* **23**, 2673 (1981).
- [14] Y. Saito, *Phys. Soc. Japan* **61**, 403 (1992); E. A. Novikov, *Phys. Rev. E* **50**, R3303 (1994).
- [15] Y. Meyer, *Ondelettes* (Hermann, Paris, 1990); I. Daubechies, *Ten Lectures on Wavelets* (S.I.A.M., Philadelphia, 1992).
- [16] C. Meneveau, *J. Fluid Mech.* **232**, 469 (1991).
- [17] R. Benzi *et al.*, *Physica* (Amsterdam) **65D**, 352 (1993).
- [18] A. Arneodo *et al.*, *J. Math. Phys. (N.Y.)* **39**, 4142 (1998); *Phys. Rev. Lett.* **80**, 708 (1998).
- [19] M. E. Cates and J. M. Deutsch, *Phys. Rev. A* **35**, R4907 (1987).
- [20] C. Meneveau and K. R. Sreenivasan, *Phys. Rev. Lett.* **59**, 1424 (1987).
- [21] P. Olla and P. Paradisi, *chao-dyn*/9803039.
- [22] A. Arneodo *et al.*, *Europhys. Lett.* **34**, 411 (1996).
- [23] J. O'Neil and C. Meneveau, *Phys. Fluids A* **5**, 158 (1993).
- [24] J.-M. Aubry and S. Jaffard, *Commun. Math. Phys.* **227**, 483 (2002).
- [25] R. H. Kraichnan, *J. Acoust. Soc. Am.* **25**, 1096 (1953); F. Lund and C. Rojas, *Physica* (Amsterdam) **37D**, 508 (1989).
- [26] C. Poulain *et al.*, *Flow, Turbul. Combust.* **72**, 245 (2004); B. Derroncourt *et al.*, *Physica* (Amsterdam) **117D**, 181 (1998).
- [27] I. Wygnanski and H. Fiedler, *J. Fluid Mech.* **38**, 577 (1969).
- [28] P. Kestener and A. Arneodo, *Phys. Rev. Lett.* **93**, 044501 (2004).
- [29] B. Dhruva *et al.*, *Phys. Rev. E* **56**, R4928 (1997).